

Spin injection in the non-linear regime: band bending effects

G. Schmidt, C. Gould, P. Grabs, A.M. Lunde,[*]

G. Richter, A. Slobodskyy, and L.W. Molenkamp

Physikalisches Institut (EP3), Universität Würzburg,

Am Hubland, 97074 Würzburg, Germany

(Dated: November 2, 2018)

Abstract

Semiconductor spintronics will need to control spin injection phenomena in the non-linear regime. In order to study these effects we have performed spin injection measurements from a dilute magnetic semiconductor [(Zn,Be,Mn)Se] into nonmagnetic (Zn,Be)Se at elevated bias. When the applied voltage is increased to a few mV we find a strong decrease of the spin injection efficiency. The observed behavior is modelled by extending the charge-imbalance model for spin injection to include band bending and charge accumulation at the interface of the two compounds. We find that the observed effects can be attributed to repopulation of the minority spin level in the magnetic semiconductor.

PACS numbers: 72.25.Dc, 72.25.Hg, 81.05.Dz

Much of our understanding of the physics of electrical spin injection from a ferromagnet into a normal metal derives from a current-imbalance model proposed by van Son[1] and, independently, by Johnson and Silsbee[2]. In this model, the current conversion is driven by a splitting of the Fermi levels for majority- and minority-spin electrons at the ferromagnet-normal metal interface. The concomitant reduction of the conductivity of the normal metal due to the suppression of a spin-channel leads to a discontinuity of the average electrochemical potential, which is sometimes referred to as the spin-induced boundary resistance. The model was put on a solid (Boltzmann) basis by Valet and Fert[3] and proved very useful for describing important spin transport phenomena including CPP-GMR (giant magnetoresistance in the current-perpendicular-to-plane geometry)[4].

In a further application, we used the model to describe spin injection into semiconductors[5], revealing the importance of a conductance mismatch between ferromagnetic metals and semiconductor. The conductance mismatch keeps the splitting of the spin-dependent Fermi levels at minimum, thus precluding spin injection. In the meantime, several methods of avoiding the conductivity mismatch have been proposed. However, by far the most robust route towards spin injection to date[6, 7] is the use of dilute II-VI magnetic semiconductors (DMSs) that exhibit the giant Zeeman effect[8], have a conductivity comparable to that of non-magnetic semiconductors, and can boast spin polarizations close to 100 % at a small applied magnetic field.

Recently, we used a simple DMS - non-magnetic semiconductor (NMS) heterostructure (consisting of (Zn,Mn,Be)Se as DMS and lattice matched (Zn,Be)Se as NMS) to demonstrate[7] the field dependence of the spin-induced boundary resistance, which increases with field as the magnetization of the paramagnetic DMS increases. The experiments reported in Ref. [7] were all done in the regime of linear response, where the current-imbalance model is appropriate.

However, spin injection experiments in semiconductors allow one to very easily enter the regime of non-linear response, where corrections to the current-imbalance model are necessary. These corrections will be manifest in any future spintronic semiconductor device, and it is thus of importance to identify them correctly.

In this paper we report on spin-injection measurements in the non-linear regime. More specifically, we experimentally demonstrate the strong effects that band-bending and charge-accumulation have on the non-linear transport. We present a modelling of the observed

phenomena which generalizes the charge-accumulation model to include the limited screening available in semiconductor structures, and shows good agreement with the experiments. It should be noted that the effects discussed here involve non-linearities influencing the spin polarization at the DMS/NMS interface, and thus are of a fundamentally different nature than the drift-induced effects discussed recently by Yu and Flatté[9] (which occur at higher electric fields).

The devices on which the experiments were carried out consisted of an all II-VI semiconductor heterostructure fabricated by molecular beam epitaxy. The heterostructure consisted of three semiconductor layers. From bottom to top these layers are a non magnetic n-type $\text{Zn}_{0.97}\text{Be}_{0.03}\text{Se}$ layer (thickness 500 nm, $n \approx 10^{19} \text{ cm}^{-3}$), a dilute magnetic $\text{Zn}_{0.89}\text{Be}_{0.05}\text{Mn}_{0.06}\text{Se}$ layer (thickness 100 nm, $n \approx 5 \times 10^{18} \text{ cm}^{-3}$) which acts as a spin aligner, and a top layer of 30 nm highly n-doped ZnSe ($n \approx 2 \times 10^{19} \text{ cm}^{-3}$). The latter was grown to ensure good quality ohmic contacts and was covered in-situ with aluminium without breaking the UHV.

In the Al-layer, $200 \times 250 \mu\text{m}$ contact pads were defined by optical lithography and wet chemical etching. These pads were used as a mask for a subsequent wet etching step through the ZnSe and the DMS down to the $\text{Zn}_{0.97}\text{Be}_{0.03}\text{Se}$. A mesa was then defined by etching down to the substrate, leaving only two contacts and the transport layer in between. The resulting sample is schematically shown as the inset in Fig. 1.

The samples were immersed in a magnetocryostat and their transport properties were determined at temperatures of 1.6 K, 3 K, 4.2 K and 6 K. The magnetoresistance of the devices was measured using dc techniques and a quasi four probe geometry, in which the wiring resistance of the setup was excluded, while the contact resistance of the device was still part of the measured resistance.[10] For bias voltages V_{bias} in the regime of linear response ($300\mu\text{V}$ or less) the device showed a positive magnetoresistance. Fig. 1 plots the relative magnetoresistance $\Delta R/R$ for a sample with a distance $x_0 = 10 \mu\text{m}$ between the contact pads, taken at 1.6 K, where the zero-field resistance $R = 420 \Omega$. As described in Ref. [7], the magnetoresistance results from the increase of the spin-induced boundary resistance with magnetic field at the two DMS/NMS interfaces in the samples. All data discussed here were taken on the same sample as that for which the low-temperature magnetoresistance is shown in Fig. 1; we verified that the effects discussed occur in samples with varying doping concentrations and dimensions. We found experimentally that both R and the saturated

magnetoresistance $\Delta R/R \approx 0.25$ are independent of temperature in the investigated range.

The main experimental result of this paper is shown in Fig.2(a). When the applied voltage is increased, a pronounced and very rapid drop of the magnetoresistance is observed, reducing the effect by two or more orders of magnitude on applying a voltage of around 10 mV across the junction. The experimental data in Fig. 2a were taken starting from three different values of $\Delta R/R$ (i.e., at different values of the magnetic field B) in the linear response regime (i.e., $\Delta R/R \approx 0.05, 0.1$ and 0.15 , respectively), at the four different temperatures mentioned above. Obviously, the non-linearities show a marked temperature dependence. Moreover, the horizontal axis displays the voltage drop over the junction V_j , rather than the total bias V_{bias} (roughly, $V_j \approx 0.15V_{\text{bias}}$), for reasons of comparison with the modelling discussed below, and because it more clearly illustrates the energy scales involved in the non-linearities. We will detail below how V_j is defined and can be calculated from V_{bias} .

The drop of the magnetoresistance can be understood if we combine the model for diffusive spin polarized transport with the band structure of the semiconductor heterostructure. When a current is driven from a spin polarized material into a non polarized material, the electrochemical potentials for spin up (μ^\uparrow) and spin down (μ^\downarrow) split at the interface. In linear response,[11] the length scale of this splitting is given by the spin scattering length of each material. The situation is depicted in Fig. 3, where the Zeeman-split conduction band (full drawn lines) and relevant potentials (dash-dotted lines) of the DMS are shown on the left side of the figure. The interface is indicated by the dotted vertical line at $x = 0$, with the NMS in the right half of the plane. The splitting of (μ^\uparrow) and (μ^\downarrow) is the driving force which leads to a spin polarized current in the non magnetic material. Because the conductivities for spin up and spin down are equal in the NMS, only a difference in the derivative of the electrochemical potential can lead to different currents in both spin channels. Since the *electrical* potential must be equal for both spin directions, this difference can only be introduced through the *chemical* potential, i.e., by spin accumulation. Spin injection thus leads to a potential drop at the interface which drives the spin conversion. This voltage drop, which may alternatively be regarded as a spin-induced boundary resistance (since it represents an extra voltage drop in the sample in absence of spin injection), is indicated in Fig.3 by the potential difference at $x = 0$ between the thin drawn lines, denoted $\mu_{\text{DMS}}^{\text{av}}$ and $\mu_{\text{NMS}}^{\text{av}}$, that extrapolate the voltage drop in the bulk of the material towards the interface.

While in the NMS the splitting of the Fermi levels is symmetrical because the conduc-

tivities for spin up and spin down electrons are identical, in the DMS, the splitting for the majority- ($c^\uparrow \equiv \mu_{\text{DMS}}^\uparrow(0) - \mu_{\text{DMS}}^{\text{av}}(0)$) and the minority- ($c^\downarrow \equiv \mu_{\text{DMS}}^{\text{av}}(0) - \mu_{\text{DMS}}^\downarrow(0)$) spin electrons can, in a one-dimensional model, be expressed as[7, 12]

$$c^\uparrow, c^\downarrow = -\frac{\lambda_{\text{NMS}}}{\sigma_{\text{NMS}}} \frac{I\beta(\beta \pm 1)}{(1 + e^{-\frac{x_0}{\lambda_{\text{NMS}}}} + 2\frac{\lambda_{\text{NMS}}}{x_0} e^{-\frac{x_0}{\lambda_{\text{NMS}}}}) + \frac{\lambda_{\text{NMS}}\sigma_{\text{DMS}}}{\sigma_{\text{NMS}}\lambda_{\text{DMS}}}(1 - \beta^2)} \quad (1)$$

where in the numerator the plus(minus) sign applies to c^\downarrow (c^\uparrow), respectively. In Eq. 1, λ_{DMS} , λ_{NMS} , σ_{DMS} , σ_{NMS} , are the spin flip length and the conductivity in the DMS and the NMS respectively, x_0 is the spacing between the contacts, I is the current and β is the degree of spin polarization in the bulk of the contacts. Note that c^\uparrow and c^\downarrow are defined setting $\mu_{\text{DMS}}^{\text{av}}(0)$ as reference level for the energy scale, i.e. $\mu_{\text{DMS}}^{\text{av}}(0) = 0$. For the potential drop ΔU at the interface, and the resulting magnetoresistance we simply have:

$$\Delta U = \mu_{\text{DMS}}^{\text{av}}(0) - \mu_{\text{NMS}}^{\text{av}}(0) = (c^\uparrow + c^\downarrow)/2, \quad (2a)$$

$$\Delta R = \Delta U/I. \quad (2b)$$

Eqs. 1 and 2 are quite general and describe spin injection in metals as well as semiconductors - but only in the linear regime. The magnitude of the Fermi-level splitting (and thus of ΔU) is different for different types of junctions: since the spin-polarized current is driven solely by the spin accumulation, the Fermi-level splitting has to be of the order of the current imbalance between the spin channels times the resistivity of the normal metal. When the magnet and the non magnet are both metals, as, e.g., in CPP GMR[4], the splitting remains small even for high currents due to the high conductivity. When the magnet is metallic and the non-magnet is a semiconductor, the splitting is determined by the material with the highest conductivity, and thus is also small. This effect leads to negligible levels of spin injection [5], and is also known as the conductance mismatch. When magnet and non magnet are both semiconductors as in the large magnetoresistance effect[7] discussed here, the splitting can easily be in the range of mV.

In a magnetic metal the Fermi energy is typically of the order of a few eV. A Fermi-level splitting of a few μV at the interface will thus not influence the properties of the magnet, and one expect the linear regime to hold up to quite high current densities. In a DMS the

situation is completely different. The Fermi energy, the Zeeman splitting, and the Fermi level splitting are in all the range of mV, and non-linear effects are to be expected when bias voltages of similar magnitude are applied.

This situation, applied to the present experiment, is pictured in some detail in Fig. 3. The conduction band of the NMS is some tens of mV below the conduction band of the DMS. The conduction band level of the DMS is split by the Zeeman splitting into two subbands, $E_{C\downarrow}^{\text{DMS}}$ and $E_{C\uparrow}^{\text{DMS}}$. From previous spin injection experiments[6, 7] and from spin flip Raman scattering we know that the DMS is fully spin polarized at low temperatures and moderate magnetic fields, which recent band structure calculations understand as resulting from the formation of an impurity band.[13] This implies that the Fermi energy is situated above the lower and at least a few mV below the upper Zeeman level.

As discussed above, spin injection will lead to the occurrence of a 'built-in potential' ΔU at the interface. This is an actual electrochemical potential step (i.e., not spin-dependent). In order to preserve both charge conservation and the band offset at the junction, ΔU has to be compensated by band bending and charging at the interface. In Fig. 3, this is indicated by the dashed lines emanating from $E_{C\downarrow}^{\text{DMS}}$ and $E_{C\uparrow}^{\text{DMS}}$. (In principle, one also expects band bending at the NMS side of the junction. For clarity, we have not included this in Fig. 3, nor in the modelling we describe below. Its inclusion is straightforward.)

Thus modified, Fig. 3 satisfies all boundary conditions imposed by the band structure and the continuity equations for the spin-polarized currents at the interface and for the total current throughout the device. However, it is now obvious that the properties of the DMS can be seriously affected by the band bending. At the interface, the majority spin electrochemical potential μ^\uparrow now approaches the upper Zeeman level $E_{C\downarrow}^{\text{DMS}}$. From the strong temperature dependence observed for the LMR effect in Ref. [7] we know that this energy gap is small enough to strongly influence the population of the upper Zeeman level and thus the bulk spin polarization β in the DMS, even at low temperatures. β being close to one, however, is a prime prerequisite for injecting a highly spin polarized current into the NMS. We can thus expect the spin polarization injection (and thus the LMR effect) to collapse as soon as the band bending starts to reduce β .

Since β and ΔU depend on each other, a modelling of the phenomena as a function of applied bias voltage should be done in a self-consistent manner. However, one can formulate a mathematically consistent description when starting from a given value of $\Delta R/R$ in the

linear response regime (this is the main reason for presenting the data emanating from the same $\Delta R/R$ value in Fig. 2.) We first use Eqs. 1 and 2 to calculate the bulk polarization β in the DMS. In the linear regime, the bulk value of β equals $\beta(x = 0)$, the spin polarization at the interface. Assuming Boltzmann statistics, we then directly have the energy splitting between $E_{C\downarrow}^{\text{DMS}}(0)$ and $\mu^\uparrow(0)$ from

$$\beta(x = 0) = \tanh((E_{C\downarrow}^{\text{DMS}}(0) - \Delta U - \mu^\uparrow(0))/2k_{\text{B}}T), \quad (3)$$

where of course $\Delta U = 0$ for infinitesimally small bias. For modelling the dependence on V_{bias} , we gradually increase ΔU (note that at this point we assume all band-bending to occur in the DMS), calculate the reduced $\beta(x = 0)$ using Eq. 3, and substitute this value for the bulk polarization in Eqs. 1 and 2 to calculate $\Delta R/R$. At the same time, ΔU can be converted in a voltage drop across the junction, V_j .

The latter quantity is conveniently accessible for comparison with the experiment. This is because $\Delta R \rightarrow 2\lambda_{\text{NMS}}/\sigma_{\text{NMS}}$ for $B, (x_0/\lambda_{\text{NMS}}) \rightarrow \infty$, as can easily be verified from Eqs. 1 and 2. Experimentally, we have (within our 1-dimensional modelling) $\sigma_{\text{NMS}} = 2.5 \times 10^{-4}\Omega^{-1}\text{cm}$, yielding $\lambda_{\text{NMS}} = 1.25\mu\text{m}$. For both the experimental (Fig. 2a) and theoretical (Fig. 2b) plots of the non-linear behavior, we may now calibrate the voltage axis according to $V_j = I\Delta R + V_{\text{bias}}(\lambda_{\text{NMS}}/x_0)$.

As to the remaining parameters in our model, we have from experiments on single DMS layers that σ_{DMS} , converted to the 1-dimensional model equals $1.0 \times 10^{-4}\Omega^{-1}\text{cm}$. The only free parameter now left in the model is λ_{DMS} . Since there is no easy method to measure λ_{DMS} , and moreover its magnetic field dependence is unknown, we simply have set the ratio $\lambda_{\text{NMS}}\sigma_{\text{DMS}}/\sigma_{\text{NMS}}\lambda_{\text{DMS}}$ in Eqs. 1 equal to 1, yielding $\lambda_{\text{DMS}} = 0.5\mu\text{m}$.

The modelling of the band bending effect as described above leads to the plots shown in Fig. 2b. We find that indeed a few mV of voltage drop across the junction are enough to reduce the spin polarization of the injected current to almost zero. The computed curves closely resemble the experimental results in shape, magnitude, voltage range, and temperature dependence, and confirm the validity of the modelling discussed above.

At this point, we should address the drift effects introduced by Yu and Flatté[9], that also can induce a reduction of $\Delta R/R$ in our experiments. For the highly (i.e., above the metal-insulator transition) doped samples used here, it is easy to show that drift effects can

only be expected for much higher electric fields than those needed to actually observe the non-linearities. Moreover, within the drift model one would not expect any temperature dependence for degenerate semiconductors, again in contradiction with the experiments. We do, however, have some indications that drift effects actually occur in certain ranges of operation. Note, e.g., that $\Delta R/R$ is not completely suppressed for high V_j in the modelling curves of Fig. 2b, while experimentally $\Delta R/R$ vanishes entirely. The drift mechanism can actually explain this behavior, be it for fields that are an order of magnitude larger than those needed to induce the initial non-linearities.

In conclusion, we have shown that when spin injection into semiconductors is used beyond the regime of linear response, the splitting of the electrochemical potentials can influence the band bending in spin-injecting junction. For finite 'built-in potentials' ΔU it is important that the energy difference ($E_{C\downarrow}^{\text{DMS}} - \mu^\uparrow(0)$) is kept sufficiently large to ensure large spin polarization at the interface. This observation may seriously limit the operational voltage of spintronic devices and forbid applications in power electronics. Appropriate tailoring of the band structure may be possible to circumvent the problems described here.

We acknowledge the financial support of the Bundesministerium für Bildung und Forschung, the DFG (SFB 410) and the DARPA SPINS program. We would like to thank V. Hock for device fabrication, and M. Flatté, K. Flensberg, and E. Rashba for useful discussions.

[*] Present and permanent address: Ørsted Laboratory, Niels Bohr Institute, DK-2100 Copenhagen, Denmark.

- [1] P. C. van Son, H. van Kempen, P. Wyder, Phys. Rev. Lett. **58**(21), 2271 (1987)
- [2] M. Johnson, and R.H. Silsbee, Phys. Rev. B **35**, 4959 (1987); Phys. Rev. Lett. **60**, 377 (1988).
- [3] T. Valet, and A. Fert, Phys. Rev. B **48**, 7099 (1993).
- [4] W.P. Pratt, Jr., S.F. Lee, J.M. Slaughter, R. Loloee, P.A. Schroeder, and J. Bass, Phys. Rev. Lett. **66**, 3060 (1991); M.A.M. Gijs, S.K. Lenczowski, and J.B. Giesbers, Phys. Rev. Lett. **70**, 3343 (1993); A. Fert, J.-L. Duvail, and T. Valet, Phys. Rev. **52**, 6513 (1995).
- [5] G. Schmidt, D. Ferrand, L. W. Molenkamp, A. T. Filip, B. J. van Wees, Phys. Rev. B **62**, R4790 (2000).

- [6] R. Fiederling, M. Keim, G. Reuscher, W. Ossau, G. Schmidt, A. Waag, and L.W. Molenkamp, Nature (London) **402**, 787 (1999).
- [7] G. Schmidt, G. Richter, P. Grabs, D. Ferrand, and L.W. Molenkamp, Phys. Rev. Lett. **87**, 227203 (2001).
- [8] J. K. Furdyna, J. Appl. Phys. **64**, R29 (1988).
- [9] Z.G. Yu, and M.E. Flatté, cond-mat/0201425
- [10] Since the spin splitting is maximum at the interface and reduces appreciably within the NMS, the actual geometry used by us is necessary in order to measure the full spin-induced boundary resistance.
- [11] For larger Fermi-level splitting or higher electric field, this statement is no longer correct, and the electron transport must be modelled using a drift model as discussed in Ref. 9.
- [12] G. Schmidt, and L.W. Molenkamp, Semicond. Sci. Technol. **17**, 310 (2002).
- [13] K. Sato, H. Katayama-Yoshida, Jap. J. Appl. Phys. **40**, L651 (2001); M. Berciu, and R.N. Bhatt, Phys. Rev. Lett. **87**, 107203 (2001); C. Timm, F. Schäfer, F. von Oppen, cond-mat/0201411; M.J. Calderón, G. Gómez- Santos, and L. Brey, cond-mat/0203404.

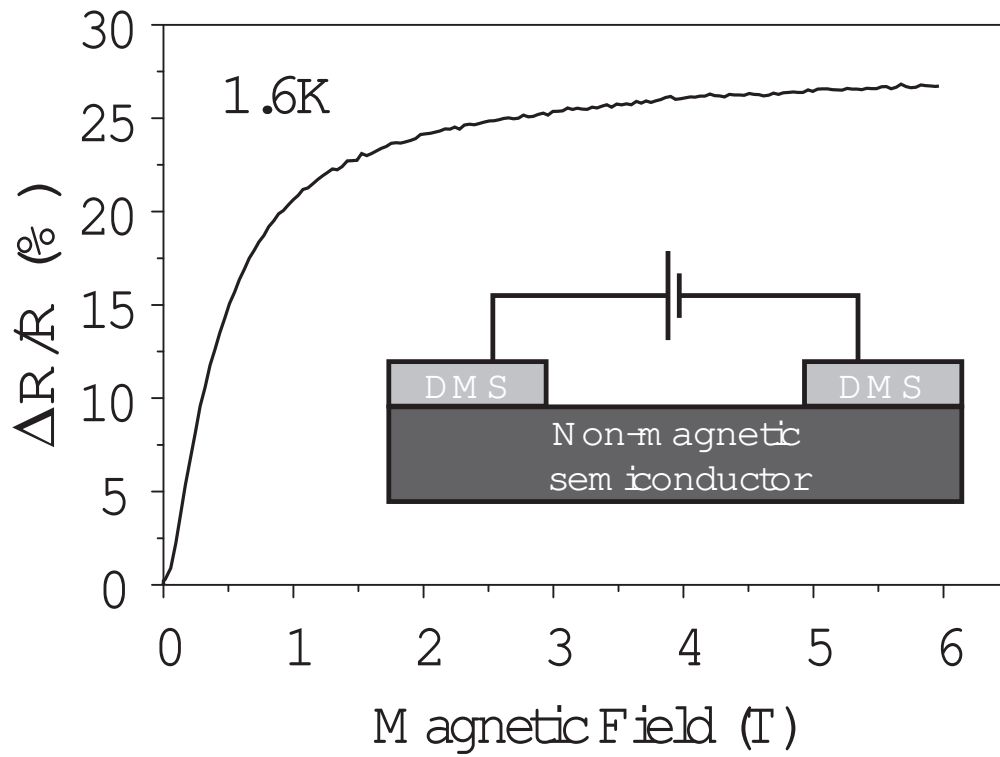


fig1 Schmidt et al.

FIG. 1: Inset: Spin injection device used in the experiment consisting of a non-magnetic semiconductor layer with two DMS top-contacts. The graph gives the resistance change $\Delta R/R$ versus magnetic field B .

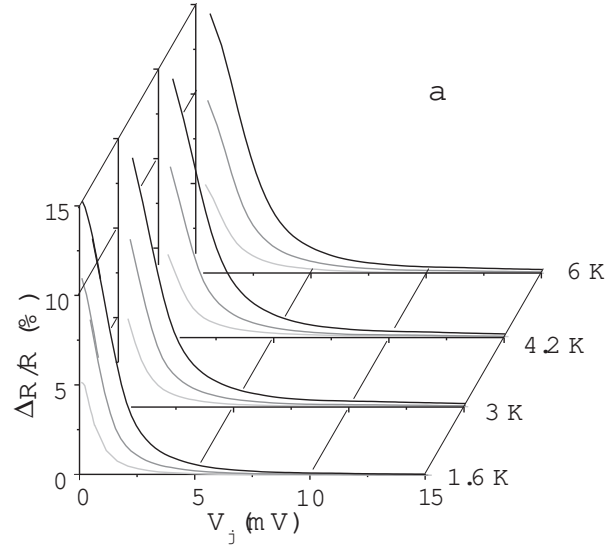


fig2a Schmidt et al.

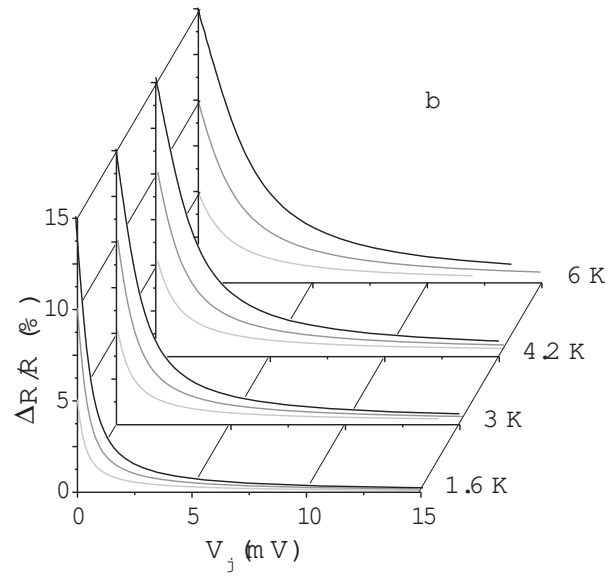


fig2b Schmidt et al.

FIG. 2: (a) Experimental and (b) theoretical non-linear magnetoresistance $\Delta R/R$ data plotted over voltage drop V_j . To facilitate comparison between experiment and theory, curves are plotted starting at several fixed values of $\Delta R/R$ (obtained by carefully adjusting B), for temperatures of 1.6, 3, 4.2 and 6 K. The parameters involved in the modelling are discussed in the text.

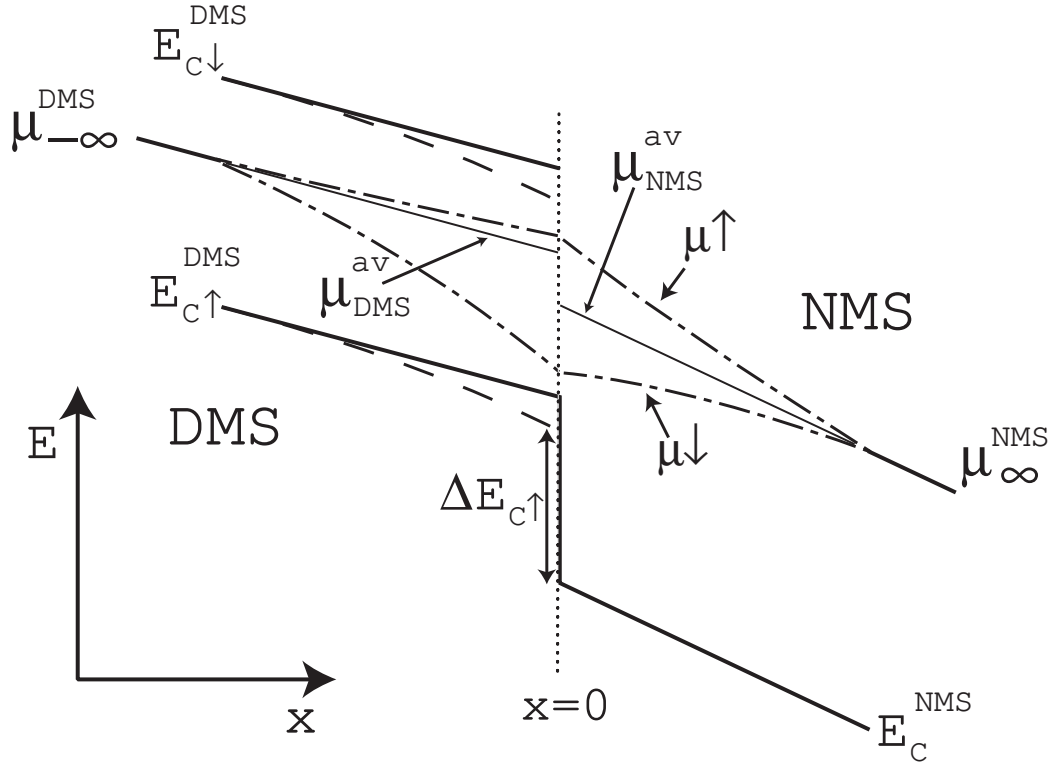


fig3 Schmidt et al.

FIG. 3: Diagram of the band bending at the spin-injecting DMS/NMS interface. $\Delta E_{C\uparrow}$ denotes the location of the conduction band offset between $E_{C\uparrow}^{\text{DMS}}$ and E_C^{NMS} when bend-bending is taken in to account; all other symbols are discussed in the text. Note the discontinuity between $\mu_{\text{DMS}}^{\text{av}}$ and $\mu_{\text{NMS}}^{\text{av}}$ at the junction ($x = 0$), which is the potential difference ΔU in Eqs. 2.